

**Development of chitosan films containing  $\beta$ -cyclodextrin inclusion complex for controlled release of bioactives.**

I. Zarandona<sup>a</sup>, C. Barba<sup>b</sup>, P. Guerrero<sup>a</sup>, K. de la Caba<sup>a\*</sup>, J. Maté<sup>b</sup>

<sup>a</sup>BIOMAT research group, University of the Basque Country (UPV/EHU), Escuela de Ingeniería de Gipuzkoa, Plaza de Europa 1, 20018 Donostia-San Sebastián, Spain.

<sup>b</sup>Department of Agronomy, Biotechnology and Food Science, Public University of Navarre (UPNa), Campus Arrosadía s/n, Edificio Los Olivos, Pamplona 31006, Spain.

<https://doi.org/10.1016/j.foodhyd.2020.105720>

© 2020. This manuscript version is made available under the CC-BY-NC-ND 4.0 license  
<http://creativecommons.org/licenses/by-nc-nd/4.0/>

\*Corresponding author: Koro de la Caba

e-mail: [koro.delacaba@ehu.eus](mailto:koro.delacaba@ehu.eus)

telephone number: +34943017188

1 **Abstract**

2 Chitosan films with antibacterial and antifungal properties have been developed with 2-  
3 phenyl ethanol. Due to the high volatility of 2-phenyl ethanol, inclusion complexes with  
4 cyclodextrins (CDs) have been prepared in order to have a controlled release of 2-  
5 phenyl ethanol.  $\beta$ -CD was selected to develop the inclusion complex since it showed  
6 higher retention yield (45 %, molar basis) than  $\alpha$ - or  $\gamma$ -CDs. Chitosan films incorporated  
7 with  $\beta$ -CD:2-phenyl ethanol were homogeneous, transparent and colorless, and  
8 showed high mechanical resistance. Furthermore, the release results of the films  
9 without the inclusion complex indicated that 2-phenyl ethanol was evaporated during  
10 the film preparation, and only an 8 % of the total bioactive was retained in the film,  
11 while the 100 % of 2-phenyl ethanol was retained in the films with the inclusion  
12 complex.

13 **Keywords:** chitosan film; inclusion complex;  $\beta$ -cyclodextrin; 2-phenylethanol.

## 14 **1. Introduction**

15 The use of active compounds is a strategy to confer functional properties, such as  
16 antimicrobial, antioxidant or UV-vis barrier properties, to films. However, many of these  
17 compounds, such as vitamins, antioxidants or flavors, are not stable under the  
18 preparation, storage and/or use conditions. Therefore, the use of encapsulation agents  
19 for active compounds become necessary to protect the compound from volatilization or  
20 possible reactions with external agents, and also to control a sustained release  
21 (Reineccius, 2009). Among encapsulation processes, spray-drying, spray-cooling,  
22 extrusion or molecular inclusion are employed in industrial processes, but only molecular  
23 inclusion occurs at molecular level and, thus, one molecule of the active compound is  
24 trapped in the cavity of the host molecule (Reineccius, Reineccius, & Peppard, 2002).  
25 The union between the active compound and the host molecule is called inclusion  
26 complex. One of these host molecules is cyclodextrin, since the Food and Agriculture  
27 Organization (FAO) of the United Nations recognizes it as additive (FAO, 2019).

28 Cyclodextrins (CD) are cyclic oligosaccharides constituted of glucose molecules joined  
29 together by  $\alpha$ -1,4 bonds. CDs are hollow truncated cone structures with an external  
30 hydrophilic character and an internal hydrophobic character (Simionato, Domingues,  
31 Nerín, & Silva, 2019; Huang, Xu, Ge, & Cheng, 2019). Therefore, it is a suitable molecule  
32 to host a variety of bioactives, including those that are non-soluble in water since  
33 interactions between cyclodextrins and guest molecules include hydrophobic forces as  
34 well as hydrogen bonding (Zhou, Lu, Zhou, & Liu, 2019).

35 Depending on the glucopyranose units conforming the molecule, the most common CDs  
36 are  $\alpha$ -,  $\beta$ - or  $\gamma$ -CDs, composed of 6, 7 or 8 glucopyranose units, respectively (Ayala-  
37 Zavala, del-Toro-Sánchez, Alvarez-Parrilla, & González-Aguilar, 2008). Due to the  
38 variety of guest molecules that can host and their acceptability as food additives, CDs  
39 are widely used in food and pharmaceutical industries. Regarding food industry, CDs  
40 can be employed for different applications, such as food supplement for spaghetti,

41 adding pumpkin oil (Durante et al., 2019), as flavor masking, reducing the high intensity  
42 of sourness, bitterness and astringency flavor in lingonberry juice (Kalanne et al., 2019),  
43 or as thermal stabilizers (Yoshikiyo et al., 2019). In the pharmaceutical industry, CDs are  
44 used to increase drug permeability, solubility and stability and to enhance organoleptic  
45 characteristics (Chantasart, & Rakkaew, 2019; Santana, Nadvorny, Passos, Soares, &  
46 Soares-Sobrinho, 2019; Yildiz, & Uyar, 2019). Regarding preparation, there are different  
47 methods for the inclusion complex preparation, such as freeze-drying, spray drying or  
48 coprecipitation (Suzuki et al., 2019).

49 CDs can be used in a variety of matrixes. Morin- $\beta$ -CD complexes have been incorporated  
50 into gelatin to prepare antioxidant films (Yuan et al., 2019). Also antimicrobials, such as  
51 citral, have been used to prepare  $\beta$ -CD inclusion complexes to preserve bioactivity during  
52 melt extrusion of EVOH films (Chen, Li, Ma, McDonald, & Wang, 2019). In order to  
53 provide films with both antioxidant and antibacterial properties, essential oils have been  
54 encapsulated into  $\beta$ -CD to promote cumulative release from chitosan films for food  
55 packaging applications (Adel, Ibrahim, El-Shafei, & Al-Shemy, 2019). In this regard,  
56 several works have been reported in relation to the use of chitosan with CD inclusion  
57 complexes for controlled release of bioactives such as resveratrol (Zhang, Cao, Ma,  
58 Chen, & Li, 2017), carvacrol (Andrade-Del Olmo, Pérez-Álvarez, Hernáez, Ruiz-Rubio,  
59 & Vilas-Vilela, 2019), or gallic acid (Munhuweyi, Caleb, Reenen, & Opara, 2018).

60 The goal of this work was to assess the effectiveness of cyclodextrin inclusion complexes  
61 as stabilizers and release controllers of 2-phenyl ethanol in chitosan films. 2-phenyl  
62 ethanol is a fragrance with a pleasant odor of rose petals (Surburg, & Panten, 1985).  
63 Although it has bacteriostatic and antifungicidal character, it is very volatile and highly  
64 susceptible to oxidation, thus, storing and keeping it stable is a troublesome (Qiu, Tian,  
65 Yin, Zhou, & Zhu, 2019; Yadav, & Lawate, 2011). Therefore, 2-phenyl ethanol has been  
66 trapped into  $\alpha$ -,  $\beta$ -, and  $\gamma$ -CDs in order to characterize and compare the retention yield.  
67 Additionally, chitosan films with  $\beta$ -CD:2-phenyl ethanol were developed and the optical,

68 physicochemical and mechanical properties of the films were characterized. In order to  
69 assess if the addition of the inclusion complex alters the properties of the film, neat  
70 chitosan and chitosan with 2-phenyl ethanol films were prepared. Furthermore, the  
71 release of 2-phenyl ethanol from chitosan films into a fatty food simulant was determined.

## 72 **2. Materials and methods**

### 73 2.1. Materials

74 Chitosan (CHI), with a molecular weight of 375 kDa and a deacetylation degree above  
75 75 %, was supplied by Sigma-Aldrich, Spain. Acetic acid and glycerol (GLY), used as  
76 solvent and plasticizer, respectively, were supplied by Panreac, Spain. 2-phenyl ethanol  
77 and  $\alpha$ -,  $\beta$ - and  $\gamma$ - cyclodextrins (CAVAMAX® w6, w7 and w8, respectively), used for the  
78 development of inclusion complexes, were food grade and supplied by Wacker  
79 Chemical, Spain.

### 80 2.2. Inclusion complex preparation

81 The inclusion complexes of 2-phenyl ethanol were prepared according to Barba,  
82 Eguinoa, & Maté (2015) with some modifications. Firstly, 10 % (w/w) cyclodextrins were  
83 hydrated for 10 min; then, 2-phenyl ethanol was added in equimolar ratio and the  
84 mixture was mechanically stirred for 24 h. In order to obtain the dry powder, a B-191,  
85 Büchi spray-dryer was used at the following conditions: 100 % aspirator capacity, inlet  
86 temperature of 180 °C, and pump at 4 mL/min. The powder was collected and stored in  
87 vials at -20 °C.

### 88 2.3. FTIR analysis of $\alpha$ -, $\beta$ -, and $\gamma$ -cyclodextrin complexes

89 Fourier-transform infrared (FTIR) spectroscopy was carried out with a Nicolet Avatar 260.  
90 Inclusion complexes ( $\alpha$ -CD:2-phenyl ethanol,  $\beta$ -CD:2-phenyl ethanol, and  $\gamma$ -CD:2-phenyl  
91 ethanol), cyclodextrins ( $\alpha$ -CD;  $\beta$ -CD and  $\gamma$ -CD) and 2-phenyl ethanol were milled with

92 anhydrous KBr and the pellet was formed by compression. The spectra were recorded  
93 between 4000-800  $\text{cm}^{-1}$  with 32 scans and a resolution of 4  $\text{cm}^{-1}$ .

#### 94 2.4. Retention of 2-phenyl ethanol cyclodextrin

95 2-phenyl ethanol was extracted from cyclodextrins by liquid-liquid extraction. 0.15 g of  
96 the inclusion complex was weighed and added into a centrifuge glass tube and 5 mL  
97 hexane and 10 mL distilled water were added. The mixture was shaken energetically for  
98 2 min and then, vortexed for 2 min. The samples were put into a bath at 85 °C and  
99 shacked for 30 min. The organic phase was gathered into a 50 mL flask. For each  
100 sample, three extractions were carried out, adding the organic phase into the 50 mL  
101 flask. A fourth extraction was done to confirm that the extraction was completed. From a  
102 1:10 solution, 1  $\mu\text{L}$  was injected into a Hewlett-Packard 5890 series II gas  
103 chromatography spectrometer (Agilent Technology, Barcelona, Spain), equipped with a  
104 flame ionization detector (FID) and a Supra Wax 280 column (1.0  $\mu\text{m}$  x 0.53 mm, 30 m).  
105 The gas carrier employed was helium, the injection temperature was 250 °C, the oven  
106 temperature program was started at 40 °C with a temperature ramp of 5 °C/min up to  
107 220 °C (1 min), and the detector temperature was set at 300 °C. In order to avoid the  
108 fluctuation of the signal, an internal standard (1-heptanol) was added to the calibration  
109 standards and samples. The retention of 2-phenyl ethanol was calculated as the ratio of  
110 experimental concentration over the theoretical content.

#### 111 2.5. Films preparation

112 Chitosan films were prepared by solution casting. 1 wt % chitosan was dissolved in 1 wt  
113 % acetic acid solution under stirring for 45 min. Then, 10 wt %  $\beta$ -CD:2-phenyl ethanol  
114 (based on chitosan) was added and stirring was continued for other 30 min. Finally, 15  
115 wt % glycerol (based on chitosan) was added as plasticizer and other 30 min of stirring  
116 were needed until total homogenization of the mixture. The solution was casted into Petri  
117 dishes and dried at room temperature for 48 h. In total, six compositions were analyzed:

118 control films, named as CHI0GLY and CHI15GLY as a function of glycerol content;  
119 chitosan films with 2-phenyl ethanol, named as CHI0GLY2PE and CHI15GLY2PE; and  
120 chitosan films with  $\beta$ -CD:2-phenyl ethanol inclusion complex, named as  
121 CHI0GLYCD:2PE and CHI15GLYCD:2PE.

## 122 2.6. Optical properties of films

123 Color and gloss parameters of the films were analyzed. Color measurements were  
124 recorded with a CR-400 Minolta Chroma Meter colorimeter (Konica Minolta, Tokyo,  
125 Japan). Ten replicates were carried out for each sample. For the determination of color  
126 parameters CIELAB scale was used: L\* from 0 to 100 (from black to white), a\* from – to  
127 + (from greenness to redness), and b\* from – to + (from blueness to yellowness).

128 Multi Gloss 268 Plus (Konica Minolta, Tokyo, Japan) was used for the determination of  
129 gloss with an incidence angle of 60° according to ASTM D523-99 (ASTM, 2018). For  
130 each composition, ten samples were assessed at room temperature.

131 Light-barrier capacity of films was measured by using a UV-VIS-NIR Shimadzu 3600  
132 spectrophotometer (Shimadzu Scientific Instruments, Kyoto, Japan) in the range of 200-  
133 800 nm.

## 134 2.7. Physicochemical properties of films

135 A Nicolet Nexus FTIR spectrometer (Thermo Fisher Scientific, Massachusetts, USA) with  
136 a Golden Gate ATR sampling accessory was employed for collecting FTIR spectra. The  
137 spectra were acquired between 4000 and 800  $\text{cm}^{-1}$  with 32 scans for each sample and  
138 a resolution of 4  $\text{cm}^{-1}$ .

139 A PANalytic Xpert Pro (PANalytical, Almelo, The Netherlands) X-ray diffraction (XRD)  
140 equipment was employed with a diffraction unit at 40 kV and 40 mA. A Cu-K $\alpha$  source  
141 was employed as radiation source and the data were collected between 2.5° and 50°.

## 142 2.8. Mechanical and barrier properties of films

143 In order to determine the tensile strength (TS), elongation at break (EAB) and Young's  
144 modulus (E), an Instron 5967 electromechanical testing system (Instron, Massachusetts,  
145 USA) was used. Samples were cut into dog bone-shaped of 4.75 mm × 22.25 mm and  
146 tests were carried out according to ASTM D1708-93 (ASTM 1993). Five replicates were  
147 tested for each sample.

148 Water vapor permeability (WVP) was tested with a PERME™ W3/0120 chamber  
149 (Labthink Instruments Co. Ltd., Shandong, China) in a controlled humidity environment,  
150 according to ASTM E96-00 (ASTM, 2000). Film discs were cut with a diameter of 7.40  
151 cm and a test area of 33 cm<sup>2</sup>. The temperature and relative humidity were set up at 30  
152 °C and 90 %, respectively. Water vapor transmission rate (WVTR) was calculated as:

153 
$$WVTR \left( \frac{g}{s \text{ cm}^2} \right) = \frac{G}{t \cdot A}$$

154 where G is the weight change (g), t is the time (s), and A is the film area that was tested  
155 (cm<sup>2</sup>).

156 WVP was calculated by the following equation:

157 
$$WVP \left( \frac{g}{cm \text{ s Pa}} \right) = \frac{WVTR \cdot L}{\Delta P}$$

158 where L is the film thickness (cm) and ΔP is the partial pressure difference of the water  
159 vapor across the film (Pa).

160 Three replicates for each sample were reported for the WVP analysis.

## 161 2.9. Bioactive release

162 Film pieces (1 cm x 2 cm) were submerged into a 95 % EtOH solution, used as a fatty  
163 food simulant (Liang et al., 2017), for 4 days under continuous stirring (200 rpm) at room  
164 temperature. Aliquots were collected at different times (30 min, 1 h, 2 h, 4 h, 8 h, 1 d, 2  
165 d, 3 d, and 4 d). The bioactive release was analyzed by using a UV-VIS-NIR Shimadzu  
166 3600 spectrophotometer (Shimadzu Scientific Instrument, Kyoto, Japan).



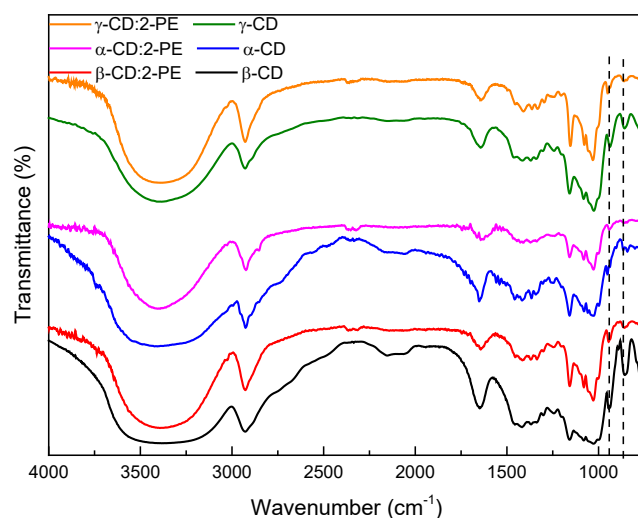
## 167 2.10. Statistical analysis

168 In order to determine significant differences among the samples, analysis of variance  
169 (ANOVA) was carried out with SPSS software (SPSS Statistics 25.0). For multiple  
170 comparisons, Tukey's multiple range test was used with a statistically significance at the  
171  $P < 0.05$  level.

## 172 **3. Results and discussion**

### 173 3.1. Characterization of $\alpha$ -, $\beta$ -, and $\gamma$ -cyclodextrin inclusion complexes

174 FTIR spectroscopy was used in order to characterize  $\alpha$ -,  $\beta$ -, and  $\gamma$ -cyclodextrin inclusion  
175 complexes with 2-phenyl ethanol. As can be seen in Figure 1, the O-H stretching  
176 vibration band is observed around  $3390\text{ cm}^{-1}$ , indicative of the hydroxyl groups of  
177 cyclodextrin. The C-O-C stretching vibrations are observed at  $1158\text{ cm}^{-1}$ , associated to  
178 the oligosaccharide structure, and the bands at  $1080$  and  $1030\text{ cm}^{-1}$  correspond to the  
179 C-C stretching vibrations of the cyclodextrin ring carbons. Additionally, the characteristic  
180 band of the  $\alpha$ -pyranyl vibration in cyclodextrin appeared at  $942.8\text{ cm}^{-1}$  and the  
181 characteristic band of  $\alpha$ -(1,4) glucopyranose in cyclodextrin appeared at  $890\text{ cm}^{-1}$  (Yuan,  
182 Ye, Gao, Yuan, Lan, Lou, Wang, 2013). As can be seen, there was no chemical  
183 interaction between the cyclodextrin and 2-phenyl ethanol. However, some characteristic  
184 bands of cyclodextrin were shifted in the inclusion complex spectra. The O-H stretching  
185 vibration displaced from  $3383\text{ cm}^{-1}$  for  $\beta$ -cyclodextrin to  $3393\text{ cm}^{-1}$  for the inclusion  
186 complex. Furthermore, C-O-C stretching vibration band moved slightly to lower  
187 wavenumbers, from  $1158\text{ cm}^{-1}$  for  $\beta$ -cyclodextrin to  $1157\text{ cm}^{-1}$  for the inclusion complex.  
188 The shift of these bands suggested physical interactions between cyclodextrins and 2-  
189 phenyl ethanol (Xiao, Hou, Kang, Niu, & Kou, 2019).



190

191 Figure 1. FTIR spectra of  $\alpha$ -,  $\beta$ -, and  $\gamma$ -cyclodextrin (CD) inclusion complexes.

192 3.2. Retention yield of 2-phenyl ethanol

193 The retention yield of 2-phenyl ethanol for  $\alpha$ -,  $\beta$ -, and  $\gamma$ -cyclodextrin inclusion complexes  
 194 was determined. The highest value was observed for  $\beta$ -cyclodextrin inclusion complex  
 195 (45 %), followed by  $\gamma$ -cyclodextrin (40 %) and finally,  $\alpha$ -cyclodextrin (32 %). These  
 196 relative low retention values can be related to the fact that 2-phenyl ethanol has only one  
 197 hydroxyl group to get attached to the cyclodextrin and, thus, the interactions could be  
 198 weaker. Regarding the differences in retention values, those differences can be  
 199 associated to the cavity size of CDs. While  $\alpha$ -cyclodextrin cavity is the smallest (5.7 Å)  
 200 to host 2-phenyl ethanol,  $\gamma$ -cyclodextrin cavity is too big (9.5 Å) and, therefore, the  
 201 interactions between the host and the guest were weaker. However,  $\beta$ -cyclodextrin cavity  
 202 (7.8 Å) was big enough to host 2-phenyl ethanol and small enough to facilitate physical  
 203 interactions between them. Taking the above into consideration, chitosan films were  
 204 prepared with the inclusion complex with the highest retention yield; therefore,  $\beta$ -  
 205 cyclodextrin:2-phenyl ethanol inclusion complexes were incorporated into chitosan film  
 206 forming solutions.

207 3.3. Optical properties of films

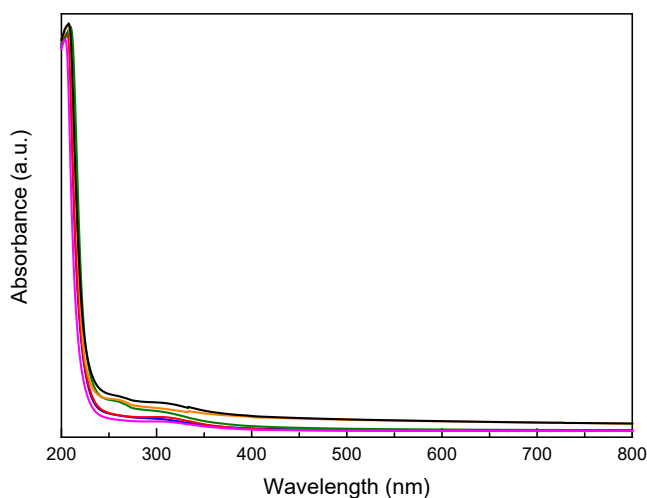
208 All films were transparent and colorless. Regarding CIELab color parameters (Table 1),  
 209 all films presented L\* values close to 100, indicating high lightness of the films; a\*  
 210 parameter values were close to zero and b\* parameters close to 3, indicating that the  
 211 films were colorless but with a greenness tendency. Considering the  $\Delta E^*$  value referred  
 212 to CHI0GLY, the films did not show differences for the naked eye, since  $\Delta E^*$  values were  
 213 lower than 1 (Uranga et al., 2019). Furthermore, statistical analysis concluded that there  
 214 were no significant difference among samples for L\*, a\* and  $\Delta E^*$  parameters, only a slight  
 215 difference for b\* value, which was not relevant. Therefore, the addition of glycerol, 2-  
 216 phenyl ethanol, or the inclusion complex did not affect the film color. Regarding gloss  
 217 values (Table 1), there was a slight increase ( $P < 0.05$ ) with the addition of 2-phenyl  
 218 ethanol or the inclusion complex, but there was no significant ( $P > 0.05$ ) difference  
 219 among the films with 2-phenyl ethanol, regardless the presence of CDs. Since gloss  
 220 values are related to the surface roughness and low values indicate rough surfaces  
 221 (Luchese, Uranga, Spada, Tessaro, & de la Caba, 2018), the values measured in this  
 222 work indicated that chitosan film surface was rough.

223 Table 1. Color (L\*, a\*, b\* and  $\Delta E^*$  parameters) and gloss values for chitosan films.

Film	L*	a*	b*	$\Delta E^*$	Gloss <sub>60</sub> (G.U.)
CHI0GLY	96.9 ± 0.5 <sup>a</sup>	-0.03 ± 0.06 <sup>a</sup>	2.5 ± 0.2 <sup>a</sup>	---	14 ± 2 <sup>a</sup>
CHI15GLY	96.6 ± 0.4 <sup>a</sup>	-0.11 ± 0.08 <sup>a</sup>	3.1 ± 0.3 <sup>b</sup>	0.6 <sup>a</sup>	16 ± 1 <sup>a</sup>
CHI0GLY2PE	96.7 ± 0.3 <sup>a</sup>	-0.08 ± 0.09 <sup>a</sup>	2.8 ± 0.2 <sup>a</sup>	0.3 <sup>a</sup>	18 ± 2 <sup>a,b</sup>
CHI15GLY2PE	96.8 ± 0.3 <sup>a</sup>	-0.11 ± 0.07 <sup>a</sup>	2.9 ± 0.2 <sup>b</sup>	0.4 <sup>a</sup>	20 ± 2 <sup>b</sup>
CHI0GLYCD:2PE	96.4 ± 0.3 <sup>a</sup>	-0.10 ± 0.04 <sup>a</sup>	2.9 ± 0.2 <sup>b</sup>	0.6 <sup>a</sup>	20 ± 1 <sup>b</sup>
CHI15GLYCD:2PE	96.4 ± 0.7 <sup>a</sup>	-0.11 ± 0.08 <sup>a</sup>	2.9 ± 0.2 <sup>b</sup>	0.6 <sup>a</sup>	20 ± 1 <sup>b</sup>

224 Two means followed by the same letter in the same parameter are not significantly  
 225 ( $P > 0.05$ ) different through the Tukey's multiple range test.

226 Additionally, UV-vis spectroscopy was carried out and results are shown in Figure 2. As  
227 can be seen, films were transparent since there was no absorption at 600 nm. In  
228 particular, there was no absorption in the visible range from 400 to 800 nm, although  
229 chitosan films absorbed UV light, especially bellow 250 nm, probably due to some  
230 chromophores present in chitosan (Leceta, Guerrero, Ibarburu, Dueñas, & de la Caba,  
231 2013).



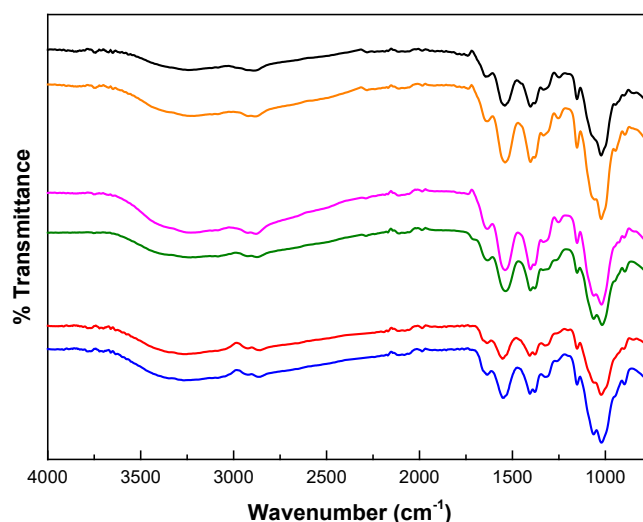
232

233 Figure 2. UV-vis light absorption of chitosan films: CHI0GLY, blue line; CHI15GLY, red  
234 line; CHI0GLY2PE, green line; CHI15GLY2PE, pink line; CHI0GLYCD:2PE, orange line;  
235 and CHI15GLYCD:2PE, black line.

### 236 3.4. Physicochemical properties of films

237 In order to assess the interactions among the components of the films, FTIR analysis  
238 was carried out and the FTIR spectra of chitosan films are shown in Figure 3. The  
239 characteristic bands of chitosan appeared at  $1630\text{ cm}^{-1}$  (amide I band), associated to  
240 C=O stretching; at  $1530\text{ cm}^{-1}$  (amide II band), related to N-H bending; and at  $1310\text{ cm}^{-1}$   
241 (amide III band) assigned to C-N stretching. Moreover, O-H stretching band and C-O-C  
242 absorption band were observed at  $3250\text{ cm}^{-1}$  and around  $1080\text{ cm}^{-1}$ , respectively. No  
243 new band was observed between the control spectra and the spectra corresponding to

244 the films with 2-phenyl ethanol, with or without CDs, indicating that no chemical reaction  
245 occurred; only slight band displacements were observed, suggesting physical  
246 interactions, such as hydrogen bonding or electrostatic interactions, among the  
247 components of the films.

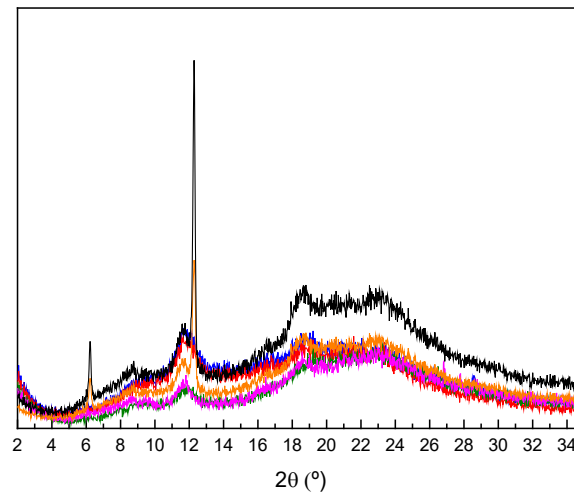


248

249 Figure 3. FTIR spectra of chitosan films: CHI0GLY, blue line; CHI15GLY, red line;  
250 CHI0GLY2PE, green line; CHI15GLY2PE, pink line; CHI0GLYCD:2PE, orange line; and  
251 CHI15GLYCD:2PE, black line.

252 In order to determine the structure of the films, XRD analysis was carried out. As can be  
253 observed in Figure 4, films without the inclusion complex present two broad peaks, one  
254 at 11.7° and another one around 21.3°, characteristic of chitosan (Pang & Zhitomirsky,  
255 2005). These broad peaks indicate the amorphous character of chitosan films. Regarding  
256 the films with the inclusion complex, two sharp peaks appeared at 6.2° and 12.3°,  
257 characteristic of  $\beta$ -cyclodextrin (Campos et al., 2019; Menezes et al., 2016), indicating  
258 the high crystallinity degree of the inclusion complex. However, the intensity of these  
259 peaks was different for the films with and without glycerol, which could be attributed to  
260 the change in molecular organization of the cyclodextrin (Campos et al., 2018). As shown  
261 by FTIR results, the intermolecular interactions with cyclodextrin molecules occurred by

262 hydrogen bonding, which changed the chitosan film structure due to the heterogeneous  
263 nucleation effect between the inclusion complex and chitosan (Li, & Zhen, 2017) and, as  
264 a consequence, the film mechanical behavior also changed.



265

266 Figure 4. XRD diffractograms of chitosan films: CHI0GLY, blue line; CHI15GLY, red  
267 line; CHI0GLY2PE, green line; CHI15GLY2PE, pink line; CHI0GLYCD:2PE, orange  
268 line; and CHI15GLYCD:2PE, black line.

### 269 3.5. Mechanical and barrier properties

270 In order to assess the effect of structure changes in the mechanical behavior, tensile  
271 tests were performed and TS and EAB values were measured and shown in Table 2. As  
272 expected, films plasticized with glycerol showed higher EAB values and lower TS and  
273 EM values, indicating more flexible and less rigid films due to the increase of free volume  
274 (Rivero, Damonte, Garcia, & Pinotti, 2016). Regarding the addition of 2-phenyl ethanol  
275 to the film forming solution, it was observed that this compound did not significantly ( $P >$   
276  $0.05$ ) change TS or EAB values with respect to the corresponding control film, probably  
277 due to the 2-phenyl ethanol evaporation during film preparation when CDs were not  
278 used. The most significant change was observed for TS values when the inclusion  
279 complex was incorporated into formulations; in particular, TS value significantly ( $P <$

280 0.05) increased from 34.5 to 48.8 MPa for the chitosan films with the inclusion complex  
 281 but without glycerol. In accordance, EM values also increased and EAB values  
 282 decreased. This behavior can be related to the interactions among chitosan and CD, as  
 283 shown by FTIR analysis, which would lead to a more compact network, increasing  
 284 resistance and rigidity, but decreasing flexibility (Siripatrawan & Vitchayakitti, 2016; Sun  
 285 et al., 2014).

286 Table 2. Tensile strength (TS, MPa), elongation at break (EAB, %), Young's Modulus  
 287 (EM, MPa) and water vapor permeability (WVP,  $\text{g}\cdot\text{cm}^{-1}\cdot\text{s}^{-1}\cdot\text{Pa}^{-1}$ ) of chitosan films.

Film	TS (MPa)	EAB (%)	EM (MPa)	WVP ( $10^{-12}\text{g}\cdot\text{cm}^{-1}\cdot\text{s}^{-1}\cdot\text{Pa}^{-1}$ )
CHI0GLY	34.5 ± 2.2 <sup>a</sup>	9.2 ± 2.2 <sup>b</sup>	1511 ± 163 <sup>a,b</sup>	1.08 ± 0.04 <sup>a</sup>
CHI15GLY	32.4 ± 3.1 <sup>a</sup>	16.4 ± 3.1 <sup>a</sup>	1374 ± 125 <sup>a</sup>	1.04 ± 0.02 <sup>a</sup>
CHI0GLY2PE	39.5 ± 3.6 <sup>a</sup>	7.8 ± 1.6 <sup>b</sup>	2205 ± 114 <sup>c</sup>	0.89 ± 0.04 <sup>b</sup>
CHI15GLY2PE	33.7 ± 3.4 <sup>a</sup>	12.3 ± 3.4 <sup>a</sup>	1687 ± 72 <sup>b</sup>	0.82 ± 0.01 <sup>b</sup>
CHI0GLYCD:2PE	48.8 ± 3.2 <sup>b</sup>	7.4 ± 2.2 <sup>b</sup>	2639 ± 173 <sup>d</sup>	0.83 ± 0.03 <sup>b</sup>
CHI15GLYCD:2PE	37.5 ± 4.1 <sup>a</sup>	8.1 ± 2.3 <sup>b</sup>	1960 ± 84 <sup>c</sup>	0.85 ± 0.02 <sup>b</sup>

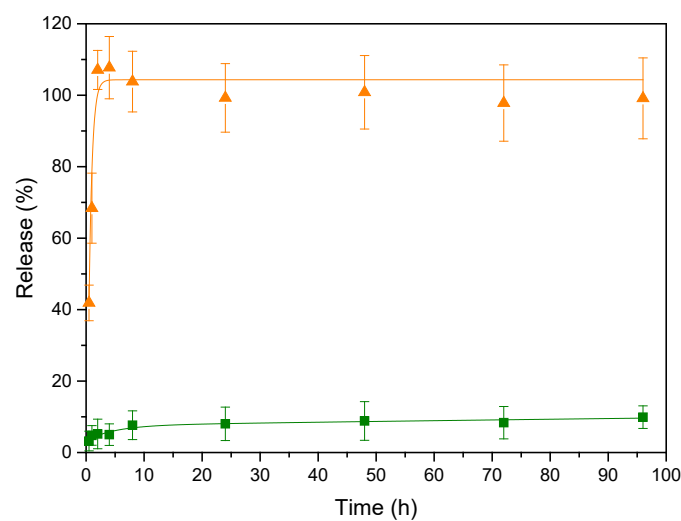
288 Two means followed by the same letter in the same parameter are not significantly  
 289 ( $P > 0.05$ ) different through the Tukey's multiple range test.

290 Regarding water vapor permeability (WVP), there was no significant difference ( $P >$   
 291  $0.05$ ) between the chitosan films without 2-phenyl ethanol. However, the addition of the  
 292 active compound significantly ( $P < 0.05$ ) decreased WVP values, probably due to the  
 293 interactions with chitosan, as shown by FTIR, and also due to the increase of  
 294 crystallinity, as observed by XRD.

### 295 3.6. Release of 2-phenyl ethanol

296 The release of 2-phenyl ethanol from chitosan films with 2-phenyl ethanol and from  
 297 chitosan films with  $\beta$ -cyclodextrin:2-phenyl ethanol were carried out in order to compare  
 298 the delivery trend during the immersion into 95 % EtOH for 4 days (Figure 5). Regarding

299 CHI0GLY2PE films, it is worth noting that some bioactive content was lost before the  
300 analysis, probably during film preparation due to the high volatility of the compound and,  
301 as a result, a maximum release of 8 % was achieved. However, chitosan films with the  
302 inclusion complex retained the bioactive inside  $\beta$ -cyclodextrin after film preparation and  
303 2-phenyl ethanol was released after 4 h of immersion into 95 % EtOH. The fast release  
304 of 2-phenyl ethanol could be explained due to the weak interactions with  $\beta$ -cyclodextrin,  
305 since 2-phenyl ethanol has only one hydroxyl group.



306

307 Figure 6. Bioactive release from chitosan films: CHI0GLY2PE, green line;  
308 CHI0GLYCD:2PE, orange line.

#### 309 4. Conclusions

310 This work showed the good capacity of cyclodextrins to form inclusion complex with 2-  
311 phenyl ethanol. Specifically,  $\beta$ -cyclodextrin showed the highest retention yield. The films  
312 obtained were homogeneous, transparent and colorless. Moreover, the addition of the  
313 inclusion complex into chitosan film forming solutions led to chitosan films with improved  
314 properties. In particular, tensile strength reached values up to 48 MPa. The tensile  
315 strength increase was related to the physical interactions between chitosan and the  
316 inclusion complex, which were corroborated by FTIR and XRD analyses, which indicated



317 the crystalline structure of chitosan films with the inclusion complex. Finally, the release  
318 of 2-phenyl ethanol into 95 % EtOH was carried out in films with and without  $\beta$ -  
319 cyclodextrin. Results suggested that the bioactive was evaporated during film  
320 preparation for the films without the inclusion complex. In contrast, the films with the  
321 inclusion complex preserved the bioactive inside the inclusion complex. These results  
322 indicated that CDs were effective to avoid the loss of bioactive compounds during film  
323 preparation.

### 324 **Acknowledgments**

325 Authors thank the Ministry of Science, Innovation and Universities (RTI2018-097100-B-  
326 C22), the Basque Government (Department of Quality and Food Industry), and the  
327 Provincial Council of Gipuzkoa (Department of Economic Development, the Rural  
328 Environment and Territorial Balance) for their financial support. Iratxe Zarandona thanks  
329 the Quality and Food Industry Department of the Basque Government for her fellowship  
330 (22-2018-00078). Also thanks are due to the Advanced Research Facilities (SGIker) from  
331 the UPV/EHU. Finally, authors would like to thank Roquette and Wacker Chemie AG for  
332 providing cyclodextrin samples.

### 333 **References**

- 334 Adel, A. M., Ibrahim, A. A., El-Shafei, A. M., & Al-Shemy, M. T. (2019). Inclusion complex  
335 of clove oil with chitosan/ $\beta$ -cyclodextrin citrate/oxidized nanocellulose biocomposite for  
336 active food packaging. *Food Packaging and Shelf Life*, 20, 100307.
- 337 Andrade-Del Olmo, J., Pérez-Álvarez, L., Hernáez, E., Ruiz-Rubio, L., Vilas-Vilela, J.L.  
338 (2019). Antibacterial multilayer of chitosan and (2-carboxyethyl)-  $\beta$ -cyclodextrin onto  
339 polylactic acid (PLLA). *Food Hydrocolloids*, 88, 228-236
- 340 ASTM D523. (2018). Standard test method for specular gloss. In *Annual book of ATSM*  
341 *standards*. Philadelphia, PA: American Society for Testing and Materials.
- 342 ASTM E96-00 (2000). Standard test methods for water vapour transmission of material,  
343 E96-00. Annual book of ASTM standards. Philadelphia, PA. American Society for  
344 Testing and Materials

345 Ayala-Zavala, J. F., del-Toro-Sánchez, L., Alvarez-Parrilla, E., & González-Aguilar, G.A.  
346 (2008). High Relative Humidity In-Package of Fresh-Cut Fruits and Vegetables:  
347 Advantage or Disadvantage Considering Microbiological Problems and Antimicrobial  
348 Delivering Systems? *Journal of Food Science*, 73 (4), 41-7.

349 Barba, C., Eguinoa, A., & Maté, J. I. (2015). Preparation and characterization of  $\beta$ -  
350 cyclodextrin inclusion complexes as a tool of a controlled antimicrobial release in whey  
351 protein edible films. *LWT-Food Science and Technology*, 64, 1362-1369.

352 Campos, C. A., Lima, B. S., Trindade, G. G. G., Souza, E. P. B. S. S., Mota, D. S. A.,  
353 Heimfarth, L., Quintans, J. S. S., Quintans-Júnior, L. J., Sussuchi, E. M., Sarmiento, V.  
354 H. V., Carvalho, F. M. S., Marreto, R. N., Costa, R. M. R., Nunes, R. S., Araújo, A. A. S.,  
355 Shanmugam, S., & Thangaraj, P. (2019). Anti-hyperalgesic and anti-inflammatory effects  
356 of citral with  $\beta$ -cyclodextrin and hydroxypropyl- $\beta$ -cyclodextrin inclusion complexes in  
357 animal models. *Life Sciences*, 229, 139-148.

358 Campos, E.V.R., Proença, P.L.F., Oliveira, J.L., Melville, C.C., Della Vechia, J.F., de  
359 Andrade, D.J., & Fraceto, L.F. (2018). Chitosan nanoparticles functionalized with  $\beta$ -  
360 cyclodextrin: a promising carrier for botanical pesticides. *Scientific Reports*, 8, 2067

361 Chantasart, D., & Rakkaew, P. (2019). Preparation and characterization of dry  $\beta$ -  
362 cyclodextrin-based ternary complexes of haloperidol and lactic acid for drug delivery.  
363 *Journal of Drug Delivery Science and Technology*, 52, 73-82.

364 Chen, H., Li, L., Ma, Y., McDonald, T. P., & Wang, Y. (2019). Development of active  
365 packaging film containing bioactive components encapsulated in  $\beta$ -cyclodextrin and its  
366 application. *Food Hydrocolloids*, 90, 360-366.

367 Durante, M., Lenucci, M. S., Gazza, L., Taddei, L., Nocente, F., De Benedetto, G. E., De  
368 Caroli, M., Piro, G., & Mita, G. (2019). Bioactive composition and sensory evaluation of  
369 innovative spaghetti supplemented with free or  $\alpha$ -cyclodextrin chlatrated pumpkin oil  
370 extracted. *Food Chemistry*, 294, 112-122.

371 Huang, Z., Xu, R., Ge, G., & Cheng, J. (2019). Complexation of capsaicin with  
372 hydroxypropyl- $\beta$ -cyclodextrin and its analytical application. *Spectrochimica Acta Part A:  
373 Molecular and Biomolecular Spectroscopy*, 223, 117278.

374 Kelanne, N., Laaksonen, O., Seppälä, T., Yang, W., Tuukkanen, K., Loponen, J., & Yang,  
375 B. (2019). Impact of cyclodextrin treatment on composition and sensory properties of

376 lingonberry (*Vaccinium vitis-idaea*) juice. *LWT - Food Science and Technology*, 113,  
377 108295.

378 Leceta, I., Guerrero, P., Ibarburu, I., Dueñas, M.T., & de la Caba, K. (2013).  
379 Characterization and antimicrobial analysis of chitosan-based films. *Journal of Food*  
380 *Engineering*, 116, 889-899.

381 Li, Y., & Zhen, W. (2017). Preparation and characterization of benzoylhydrazide-  
382 derivatized poly(lactic acid) and  $\gamma$ -cyclodextrin inclusion complex and its effect on the  
383 performance of poly(lactic acid). *Polymers Advanced Technologies*, 28, 1617-1628.

384 Liang, J., Yan, H., Zhang, J., Dai, W., Gao, X., Zhou, Y., Wan, X., & Puligundla, P. (2017)  
385 Preparation and characterization of antioxidant edible chitosan films incorporated with  
386 epigallocatechin gallate nanocapsules. *Carbohydrate Polymers*, 171, 300-306.

387 Luchese, C. L., Uranga, J., Spada, J. C., Tessaro, I. C., & de la Caba, K. (2018).  
388 Valorisation of blueberry waste and use of compression to manufacture sustainable  
389 starch films with enhanced properties. *International Journal of Biological*  
390 *Macromolecules*, 115, 955-960.

391 Menezes, P. P., Dória, G. A. A., Araújo, A. A. S., Sousa, B. M. H., Quintans-Júnior, L. J.,  
392 Lima, R. N., Alves, P. B., Carvalho, F. M. S., Bezerra, D. P., Mendonça-Júnior, F. J. B.,  
393 Scotti, L., Scotti, M. T., da Silva, G. F., de Aquino, T. M., Sabino, A. R., do Egito, E. S.  
394 T., & Serafini, M. R. (2016). Docking and physico-chemical properties of  $\alpha$ - and  $\beta$ -  
395 cyclodextrin complex containing isopulegol: a comparative study. *Journal of Inclusion*  
396 *Phenomena and Macrocyclic Chemistry*, 85, 341-354.

397 Munhuweyi, K., Caleb, O. J., van Reenen, A. J., & Opara, U. L. (2018). Physical and  
398 antifungal properties of  $\beta$ -cyclodextrin microcapsules and nanofibre films containing  
399 cinnamon and oregano essential oils. *LWT - Food Science and Technology*, 87, 413-  
400 422.

401 Pang, X., & Zhitomirsky, I. (2005). Electrodeposition of composite hydroxyapatite-  
402 chitosan films. *Materials Chemistry and Physics*, 94, 245-251.

403 Qiu, B., Tian, H., Yin, X., Zhou, Y., & Zhu, L. (2019). Microencapsulation of 2-phenyl  
404 ethanol with methylcellulose/alginate/methylcellulose as the wall material and stability of  
405 the microcapsules. *Polymer Bulletin*, 1-13.

406 Reineccius, G. A. (2009). Edible films and coatings for flavor encapsulation. In M. E.  
407 Embuscado, & K. C. Huber (Eds.), *Edible films and coatings for food applications* (pp.  
408 269-294). New York: Springer.

409 Reineccius, T. A., Reineccius, G. A., & Peppard, T. L. (2002). Encapsulation of flavors  
410 using cyclodextrins: comparison of flavor retention in alpha, beta, and gamma types.  
411 *Journal of Food Science*, 67, 3271-3279.

412 Rivero, S., Damonte, L., García, M. A., & Pinotti, A. (2016). An Insight into the Role of  
413 Glycerol in Chitosan Films. *Food Biophysics*, 11, 117-127.

414 Santana, A. C. S. G. V., Nadvorny, D., Passos, T. D. R., Soares, M. F. L. R., & Soares-  
415 Sobrinho, J. L. (2019). Influence of cyclodextrin on posaconazole stability, release and  
416 activity: Improve the utility of the drug. *Journal of Drug Delivery Science and Technology*,  
417 53, 101153.

418 Simionato, I., Domingues, F. C., Nerin, C., & Silva, F. (2019). Encapsulation of cinnamon  
419 oil in cyclodextrin nanosponges and their potential use for antimicrobial food packaging.  
420 *Food and Chemical Toxicology*, 132, 110647.

421 Siripatrawan, U., & Vitchayakitti, W. (2016). Improving functional properties of chitosan  
422 films as active food packaging by incorporating with propolis. *Food Hydrocolloids*, 61,  
423 695-702.

424 Sun, X., Siyao Sui, S., Ference, C., Zhang, Y., Sun, S., Zhou, N., Zhu, W., & Zhou, K.  
425 (2014). Antimicrobial and Mechanical Properties of  $\beta$ -Cyclodextrin Inclusion with  
426 Essential Oils in Chitosan Films. *Journal of Agricultural and Food Chemistry*, 62, 8914-  
427 8918.

428 Surburg, H., & Panten, J. (1985). *Common Fragrance and Flavor Materials. Preparation,*  
429 *Properties and Uses.* (5th ed.). Weinheim: WILEY-VCH Verlag GmbH & Co, (Chapter  
430 2).

431 Suzuki, R., Inoue, Y., Murata, I., Nomura, H., Isshiki, Y., Hashimoto, M., Kudo, Y.,  
432 Kitagishi, H., Kondo, S., & Kanamoto, I. (2019). Preparation, characterization, and study  
433 of the antimicrobial activity of a Hinokitiol-copper(II)/ $\gamma$ -cyclodextrin ternary complex.  
434 *Journal of Molecular Structure*, 1194, 19-27.

435 Uranga, J., Puertas, A. I., Etxabide, A., Dueñas, M. T., Guerrero, P., & de la Caba, K.  
436 (2019). Citric acid-incorporated fish gelatin/chitosan composite films. *Food*  
437 *Hydrocolloids*, 86, 95-103.

438 Xiao, Z., Hou, W., Kang, Y., Niu, Y., & Kou, X. (2019). Encapsulation and sustained  
439 release properties of watermelon flavor and its characteristic aroma compounds from  $\gamma$ -  
440 cyclodextrin inclusion complexes. *Food Hydrocolloids*, 97, 105202.

441 Yadav, G. D., & Lawate, Y. S. (2011). Selective hydrogenation of styrene oxide to 2-  
442 phenyl ethanol over polyuria supported Pd-Cu catalyst in supercritical carbon dioxide.  
443 *Journal of Supercritical Fluids*, 59, 78-86.

444 Yildiz, Z. I., & Uyar, T. (2019). Fast-dissolving electrospun nanofibrous films of  
445 paracetamol/cyclodextrin inclusion complexes. *Applied Surface Science*, 492, 626-633.

446 Yoshikiyo, K., Yoshioka, Y., Narumiya, Y., Oe, S., Kawahara, H., Kurata, K., Shimizu,  
447 H., & Yamamoto, T. (2019). Thermal stability and bioavailability of inclusion complexes  
448 of perilla oil with  $\gamma$ -cyclodextrin. *Food Chemistry*, 294, 56-59.

449 Yuan, L., Li, S., Zhou, W., Chen, Y., Zhang, B., & Guo, Y. (2019). Effect of morin-HP-  $\beta$ -  
450 CD inclusion complex on anti-ultraviolet and antioxidant properties of gelatin film.  
451 *Reactive and Functional Polymers*, 137, 140-146.

452 Yuan, Z., Ye, Y., Gao, F., Yuan, H., Lan, M., Lou, K., & Wang, W. (2013). Chitosan-graft-  
453  $\beta$ -cyclodextrin nanoparticles as a carrier for controlled drug release. *International Journal*  
454 *of Pharmaceutics*, 446, 191-198

455 Zhang, D., Cao, Y., Ma, C., Chen, S., & Li, H. (2017) Development of Water-Triggered  
456 Chitosan Film Containing Glucamylase for Sustained Release of Resveratrol. *Journal of*  
457 *Agricultural and Food Chemistry*, 65, 2503-2512.